Available online at www.sciencedirect.com
ScienceDirect
Icarus ••• (••••) •••–•••
ICARUS
www.elsevier.com/locate/icarus

A top-down origin for martian mantle plumes

P. van Thienen [a,*], A. Rivoldini [b], T. Van Hoolst [b], Ph. Lognonné [a]

[a] *Équipe Études Spatiales et Planétologie, Institut de Physique du Globe de Paris, 4, Avenue de Neptune, 94107 Saint-Maur-des-Fossés, France*
[b] *Royal Observatory of Belgium, 3 Avenue Circulaire, B-1180 Brussels, Belgium*

Received 23 February 2006; revised 22 June 2006

Abstract

The two main volcanic centers on Mars, Tharsis and Elysium, are often interpreted in terms of mantle plume hotspots, even though there are several problems with the plume hypothesis for Mars. We present results of 2D cylindrical shell numerical mantle convection experiments in which we try to ascertain whether flushing of the hot lower mantle could provide a mechanism for the generation of a small number of plume-like features, i.e., localized upwelling of hot material. In this scenario the formation of hot upwellings is driven from the top by cold downwellings rather than from a hot thermal boundary layer at the CMB. First we construct a range of Mars interior structure models consistent with observations in order to demonstrate that the presence of a thin lower mantle in the martian interior is a viable scenario. Then we use a series of numerical convection experiments to investigate the effects of solid-state phase transitions, different stratified and temperature-dependent viscosity models, and the presence of a thick southern hemisphere crust on the operation of such a mechanism. Our results show that it is possible to generate hot strong localized upwellings from top-down dynamics if the lithosphere is thin or actively involved in the convective pattern. The presence of a thick, immobile, insulating southern hemisphere crust reduces the number of upwellings, and the perovskite phase transition causes a focusing of the upwellings. Further experiments demonstrate that an initial 500 Myr phase of mobile lid is sufficient to start this process create an upwelling which is stable for billions of years.

Keywords: Mars, interior; Volcanism; Geophysics

1. Introduction

Though many small volcanoes are scattered over the surface of Mars, two volcanic centers distinguish themselves from the rest by their size and long-term activity up until recent times: Tharsis and Elysium. In the Tharsis region, most volcanic activity took place during the Noachian and Hesperian periods (Dohm and Tanaka, 1999). However, evidence for recent activity (up to 40–100 Myr) on several Tharsis volcanoes was found as well (Hartmann et al., 1999; Neukum et al., 2004). Activity in the Elysium region was also found to have taken place over a several billion year period (Neukum et al., 2004).

Just like hotspots on Earth are often (though not undisputedly; see, e.g., Anderson et al.,1992; Anderson, 2002) interpreted in terms of mantle plumes, these martian volcanic centers have also been interpreted as resulting from hot upwellings from the martian core–mantle boundary (e.g., Zuber, 2001; Kiefer, 2003). However, ever since the earliest numerical simulations of mantle convection in the martian mantle (e.g., Schubert et al., 1990), it has been clear that to produce only two mantle plumes in the martian mantle is not trivial.

Several explanations for the apparently small number of martian mantle plumes have been proposed. Breuer et al. (1997) investigated the effect of exothermic phase transitions on plumes in the martian mantle. They found that the consumption and release of latent heat have a much stronger impact than in the Earth because of the lower adiabatic gradient, which results in intermittent permeability of the phase transition, reducing the number of penetrating plumes. The presence of an endothermic phase transition in the deep martian mantle, the equivalent of the 670 km discontinuity in the Earth's mantle,

* Corresponding author. Present address: Institute of Geosciences, Utrecht University, P.O. Box 80.021, 3508 TA Utrecht, The Netherlands.
E-mail addresses: thienen@geo.uu.nl (P. van Thienen), rivoldini@oma.be (A. Rivoldini), tim.vanhoolst@oma.be (T. Van Hoolst), lognonne@ipgp.jussieu.fr (Ph. Lognonné).

0019-1035/$ – see front matter
doi:10.1016/j.icarus.2006.06.008

may have a significant influence on the mantle dynamics. Numerical experiments in 2D by Weinstein (1995) show that the presence of an endothermic phase transition close to the CMB may trap the thermal boundary layer and allow only a single plume to penetrate the transition. Harder and Christensen (1995) and Harder (1998) showed in 3D convection models that the presence of such a transition may reduce the number of plumes to about 2, consistent with the interpretation that Tharsis and Elysium are plume-related features. However, the time scale on which this convection pattern develops is much too long, about 8 Gyr. Harder (1998) ascribes this to the absence of decay of heat sources in the model. The presence of an endothermic phase transition in the deep martian mantle, however, depends on whether the mantle is deep enough, i.e., the size of the martian core. There is still much uncertainty about this number, with estimates ranging from less than 1300 km to more than 1700 km (Folkner et al., 1997; Yoder et al., 2003). For a core size less than about 1550 km, the presence of the endothermic phase transition may be expected (Bertka and Fei, 1998). The presence of this phase transition will be investigated and discussed in more detail below.

Classically plumes are thought to be formed at a thermal boundary layer, usually at the core mantle boundary (Cserepes and Yuen, 2000) [though the models of Harder (1998) require only a small amount of bottom heating to show the two plume characteristic mode of convection]. The presence of such a TBL during the earliest phases of Mars's evolution implies that the core was initially superheated, though at the moment this remains speculation (Breuer and Spohn, 2003; Williams and Nimmo, 2004). The apparent presence of a strong magnetic field during the first 0.5 Gyr of Mars' history (Acuña et al., 1999) suggests a strong thermal gradient across the CMB during this period. However, this does not necessarily correspond to conditions favorable for plume formation, but may also be caused by the presence of cold material on the CMB, either subducted lithosphere (Nimmo and Stevenson, 2000) or a mantle overturned due to chemical differentiation in a magma ocean (Elkins-Tanton et al., 2003). The absence of a magnetic field after this initial period suggests a relatively small heat flux out of the core, i.e., a reduced temperature contrast between core and mantle.

Wenzel et al. (2004) investigated the convective patterns of a layered martian mantle (which could result from differentiation during an early magma ocean phase; Righter et al., 1998; Kiefer, 2003) and the dichotomy. They use analog experiments to demonstrate than in such a layered system, in which the bottom of the upper layer is heated by the lower layer, upwellings form early, are focused under the southern highlands, and may persist for very long times, consistent with observations.

An external rather than an internal origin of Tharsis has been suggested by Reese et al. (2004), who investigated the possibility of impact-induced mantle plumes. They found that the impact of bolides on the order of 500–1000 km may produce localized melting events. The calculated melt volumes do a good job of matching those observed at Tharsis, but this model fails to explain (though this was not the focus of the study) the fact that volcanism at Tharsis spans a period of several billions years (Dohm and Tanaka, 1999; Hartmann et al., 1999; Neukum et al., 2004).

An explanation for the recent volcanic activity of Tharsis which does not involve plumes or upwellings was proposed by Schumacher and Breuer (2006). They calculated that the lower thermal conductivity of the thick Tharsis crust may cause a blanketing effect and allow (a larger degree of) partial melting underneath this region, removing the need for a hot upwelling.

In this paper, we present an alternative endogenic model for the formation of a small number of strong, stable, hot upwellings in the martian mantle, which does not depend on the long-term presence of a thermal boundary layer at the core mantle boundary. We investigate, by using numerical experiments, under which conditions the flushing of the lower mantle (if an endothermic phase transition is present) is capable of generating a small number (1 or 2) focused hot upwellings. To make sure we are studying this effect only, bottom heating is explicitly excluded. We look at the effects of the dichotomy, phase transitions, and the viscosity model on the operation of this process. First we discuss the evolution of the thermal state of Mars, and the possibility of forming plume-like features without a thermal boundary layer. Then we investigate to what extent presently available data allow the presence of a perovskite layer, and we continue to present our numerical convection model and its results. It is not our intention to present this process as a unique mechanism which rules out the (simultaneous) operation of any other process like hot TBL plumes. However, we will argue that in the case of Mars, this process may be important for understanding how the planet works.

2. Mars' thermal state and its evolution

It is generally assumed (e.g., Righter et al., 1998; Elkins-Tanton et al., 2003) that Mars had a magma ocean during its earliest history although numerical models by Senchu et al. (2002) suggest this may not have been the case at all. In scenarios which do include a magma ocean, cooling from the top results in a shift of the lower boundary of the magma ocean to shallower levels (Abe, 1997; Solomatov, 2000). As $\mathrm{d}T/\mathrm{d}p$ of the solidus is greater than the adiabatic gradient, the mantle which solidifies below the magma ocean will be convectively instable and convect toward an adiabatic gradient [similar to the argument of Solomatov (2000) for Earth's late stage accretion geotherm]. As soon as the magma ocean has disappeared [Abe (1997) has calculated that for Earth, this may take 100–200 Myr, but for Mars it will probably be less], cold downwellings from either the bottom of the lithosphere (stagnant lid regime) or from the surface (active surface tectonics) can sink into the deeper mantle, increasing temperature variations and therefore the vigor of convection.

Evidence from martian meteorites indicates that the martian core was probably formed very rapidly, within 20 Myr of Solar System formation (Halliday et al., 2001). The question of the initial thermal structure of the martian mantle is closely connected to the question of initial superheating of the core, which is expected (e.g., Williams and Nimmo, 2004) but has not yet been demonstrated.

Please cite this article as: P. van Thienen et al., A top-down origin for martian mantle plumes, Icarus (2006), doi:10.1016/j.icarus.2006.06.008.

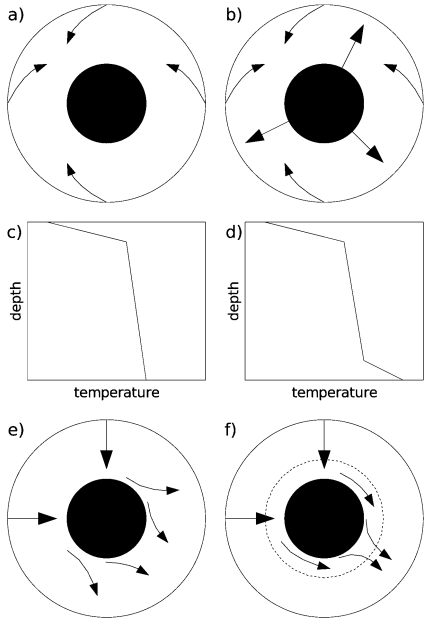

Fig. 1. Two scenarios for the initiation of mantle dynamics after magma ocean crystallization. (a) Core is initially not superheated. (b) Core is initially superheated relative to the mantle. The corresponding areotherms are shown in (c) and (d). Passive upwelling driven by active downwelling is unfocused in the absence of a mantle phase transition (e), but may be focused if this transition is present (f).

In the magma ocean free scenario of Senchu et al. (2002), initially a three-layer planet is formed, containing a cold, undifferentiated core, a layer of liquid metal capable of producing a dynamo, and a hot differentiated outer silicate layer. Since this configuration is gravitationally unstable, an overturn must take place which results in the formation of a metallic core. Senchu et al. (2002) predict that this process may take 0.5–1 Gyr. It appears likely that in this scenario the core (originally a hot liquid metal layer) ends up being superheated relative to the mantle (mixture of hot silicate outer layer and undifferentiated interior) after this overturn process.

This leads to two possible scenarios for the initiation of dynamics in the solid martian mantle. In the first scenario, where there is no initial temperature contrast between the core and the mantle, large-scale dynamics are initiated from the top down (Fig. 1a,c). In the second scenario (Fig. 1b,d), the martian core is initially superheated, dynamics are initiated both top-down (cool downwellings from the base of the lithosphere or the lithosphere itself) and bottom-up (plumes from the thermal boundary layer at the CMB).

Obviously these two scenario's present simplifications. The freezing of the magma ocean is not a sudden event, and chemical differentiation during the cooling of the magma ocean may produce an unstable density stratification which could result in a mantle overturn (Elkins-Tanton et al., 2003). Whereas the former point may not present too much of a problem for these scenario's, the latter would possibly invalidate them completely, so we need to keep this in mind.

At this moment it is not clear which of the scenarios is preferable. In this paper, the models investigated correspond to the first scenario, without initial core superheating, in terms of the resulting dynamics. However, Mars cooling models suggest that an initially superheated core is likely to cool to near-mantle temperatures in some hundreds of millions of years (Breuer and Spohn, 2003), probably long before the start of large-scale magmatic activity at Tharsis. Therefore, our results may also be representative for the second scenario after an initial phase in which the core was superheated.

As mentioned in the Introduction, the presence of a magnetic field during the first 500 Myr and its absence afterwards suggest a strong temperature contrast between core and mantle during this initial period and a reduced contrast after. The initially strong contrast can be explained either by an initially superheated core or by the positioning of cold material from the surface close to the core mantle boundary. It's reduction later on suggests that bottom-up dynamics such as plumes from a thermal boundary layer may not have been so important during most of the planet's history. The parametric models of Breuer and Spohn (2003) show a CMB heat flow between -5 (into the core) and $+5$ mW m^{-2} for most of their scenarios, even in cases with an initial temperature difference of 250 K between core and mantle (see their Figs. 7 and 9). The thermal evolution models of Nimmo and Stevenson (2000) show similarly low heat fluxes at the CMB, which may be negative (i.e., into the core) for significant portions of the evolution, specifically when an initial period of plate tectonics is modeled. Therefore, the TBL plume interpretation does not appear to be consistent with several Gyr of volcanic activity in Tharsis and Elysium.

3. Hot upwellings without a thermal boundary layer

Several studies, applied to the Earth, have shown that the presence of an endothermic phase transition may result in (partially) layered convection (e.g., Christensen and Yuen, 1985). The piling up of cold downwelling material on the phase transition may force a sudden breakthrough or 'avalanche' of this cold material (Machetel and Weber, 1991; Tackley et al., 1993). As a counterflux, hot lower mantle material flows into the upper mantle. In their models, these events are generally quite catastrophic. Cserepes and Yuen (2000) suggested that this process may also take place on a smaller scale, resulting in plume-like features (in the sense of hot mushroom-shaped mantle diapirs) which do not originate from a thermal boundary layer. Similar features were also observed in thermo-chemical mantle convection models applied to the early Earth of Van Thienen et al. (2004a). In this scenario, the phase transition causes focusing the upwards counterflow to the downwellings (Fig. 1e,f). We propose this type of features may be responsible for the formation of Tharsis and Elysium.

4. Does Mars have a perovskite lower mantle?

A perovskite lower mantle in Mars only exists if the pressure and temperature in the mantle increase to values high enough for the phase transition to perovskite to take place. Both the temperature profile in the mantle (Breuer and Spohn, 2003) and the experimental determination of the temperature of the phase transition as a function of pressure are uncertain by a few 100 K

Please cite this article as: P. van Thienen et al., A top-down origin for martian mantle plumes, Icarus (2006), doi:10.1016/j.icarus.2006.06.008.

(Figs. 2 and 3). To verify whether, given these uncertainties, the phase transition to perovskite can occur in the martian mantle, we have constructed Mars interior structure models that satisfy recent geophysical data and mantle temperature profiles resulting from thermal evolution models. In particular, the mean planetary density, obtained from the planet's mass and size, the polar moment of inertia C (Yoder et al., 2003) and the tidal Love number k_2 (Yoder et al., 2003) give important constraints on the interior structure of a planet, if a given mantle thermal state and a bulk composition is specified.

To determine the interior structure models we followed the method developed by Rivoldini et al. (in preparation). The models have three chemically homogeneous reservoirs: the crust, the mantle (with possible phase transitions) and the core. The mantle composition modeling used is described in Verhoeven et al. (2005). Here we consider two mantle mineralogy compositions: the model of Bertka and Fei (1997) derived from Dreibus and Wanke's (1985) study of SNC meteorites and the model EH45 from Sanloup et al. (1999). Further, we consider two temperature profiles corresponding to plausible end-members of thermal evolution models from Breuer and Spohn (2003). The hot temperature profile implies less dense mantles, larger cores and lower pressures at the core mantle boundary, whereas the models with the colder areotherm have denser mantles, smaller cores and higher pressures at the core mantle boundary. The bulk core is assumed to be composed of Fe, Ni (7.6 wt%) and S. It is widely assumed (Longhi et al., 1992) that the core sulfur content x_s is about 14 wt%. In our modeling we allow for 10 wt% $< x_s <$ 17 wt%, a range enclosing the value of 14.2 wt% derived by Dreibus and Wanke (1985). The core is made of γ-Fe, Ni and FeS V. The assemblage is brought to Mars core (P, T) conditions by means of the Birch–Murnaghan equation of state (Sohl and Spohn, 1997). To account for the liquid phase, the computed density values at (P, T) are decreased by about 2%. The spherically symmetric models are constrained by the radius, the mass, and the mean moment of inertia I. The moment of inertia factor $I/MR^2 = 0.3635 \pm 0.0012$ is computed from the polar moment of inertia C and the accurately known gravity coefficient J_2, and includes a correction for the Tharsis rise (Sohl et al., 2005).

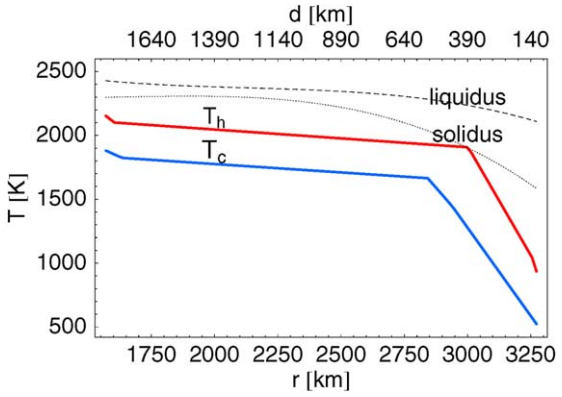

Fig. 2. Mars mantle areotherms used for the construction of Mars interior models.

The pressure and temperature conditions at the core mantle boundary of our models are close to the phase transition values (Fig. 3). Because sufficiently large pressures are needed for the perovskite phase transition to take place, it could be expected that mainly the colder models, with larger core mantle boundary pressures, could have this phase transition. However, most experimental data on the perovskite phase transition show that the transition for higher temperatures occur at lower pressures, and both hot and cold models with a perovskite layer are possible. Fig. 4 shows the same results, plotted in k_2–P_{cmb} space. Models that satisfy the estimates of the tidal Love num-

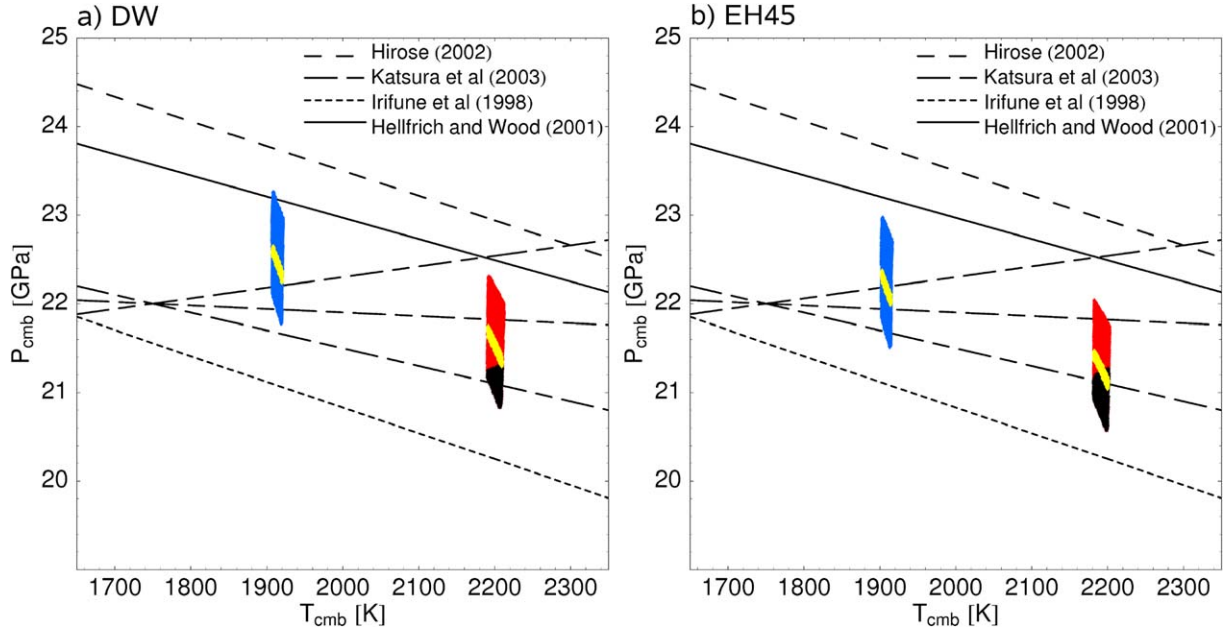

Fig. 3. Position of perovskite phase transition according to several authors superposed on the core pressure and temperature domains of the cold (dark grey) and hot (light grey) mantle interior models lying within the range of the moment of inertia uncertainties. Models which have a sulfur concentration of about 14 wt% S in the core are represented by the shaded area, models that lie within the uncertainties of the latest k_2 estimates are represented by the black shaded area.

Please cite this article as: P. van Thienen et al., A top-down origin for martian mantle plumes, Icarus (2006), doi:10.1016/j.icarus.2006.06.008.

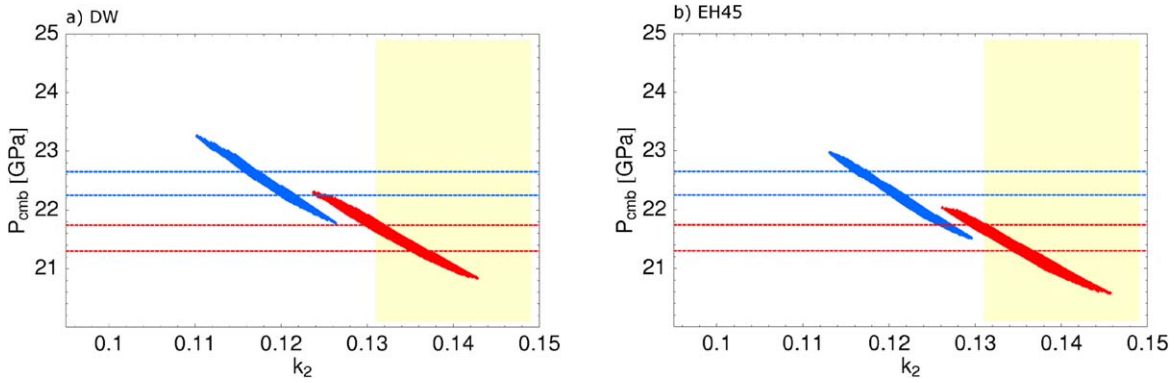

Fig. 4. Core mantle boundary pressure as a function of Love number k_2 for the hot (light grey) and cold (dark grey) mantle temperature profile for the DW (a) and EH45 (b) mantle compositions. Mars core's that have about 14 wt% sulfur have P_{cmb} values in the range delineated by the dashed lines. The k_2 values in the shaded area are those of the official MGS95J solution.

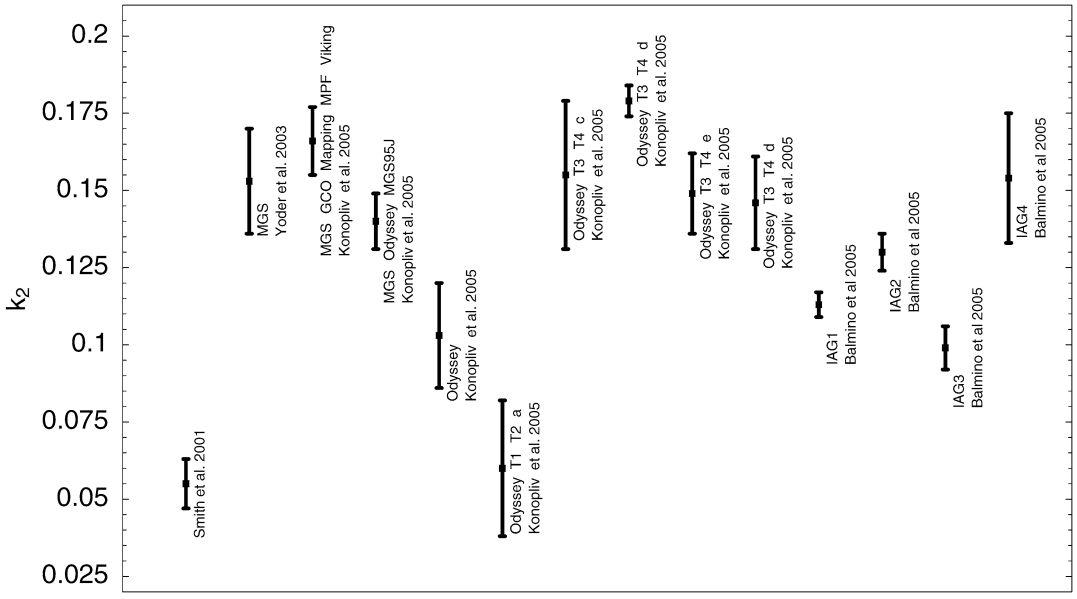

Fig. 5. Overview of recently published values for Mars' k_2 Love number. Cited papers are: Smith et al. (2001), Yoder et al. (2003), Balmino et al. (2005), Konopliv et al. (2006).

ber $k_2 = 0.153 \pm 0.017$ (Yoder et al., 2003) can only have a perovskite layer if the phase transition occurs at the lower end of the experimental data for the pressures at the phase transition (Fig. 3). Considering the error bounds, this value is marginally consistent with geochemistry, as all acceptable models with a core sulfur content between 10 and 17 wt% in Fig. 4 correspond to k_2 values between 0.11 and 0.145. Most more recent computations range between Yoder's value and a significantly lower value around 0.10, as is illustrated in Fig. 5.

5. Numerical convection model

In order to test the plausibility of our hypothesis, we apply a 2D cylindrical shell convection code, based on the finite element package SEPRAN (Segal and Praagman, 2002). Infinite Prandtl number is assumed, allowing us to disregard inertial terms. The governing equations, taking into account conservation of energy, momentum, and mass, are considered in the framework of the extended Boussinesq approximation. The corresponding (non-dimensionalized) expressions are:

$$\frac{\partial T}{\partial t} + u_j \partial_j T - Di(T + T_0)w = \partial_j \partial_j T + \frac{Di}{Ra}\Phi + \sum_k \gamma_k \frac{Rb_k}{Ra} Di(T + T_0)\frac{\mathrm{d}\Gamma_k}{\mathrm{d}t} + RH, \quad (1)$$

$$\partial_j \tau_{ij} - \partial_i \Delta p - \left(Ra\, T - \sum_k Rb_k \Gamma_k\right) = 0, \quad (2)$$

$$\partial_j u_j = 0. \quad (3)$$

The thermal and phase Rayleigh numbers Ra and Rb_k (for phase transition k) representing the driving force of convection are defined as

$$Ra = \frac{\rho_0 g \alpha \Delta T h^3}{\eta_0 \kappa} \quad (4)$$

and

$$Rb_k = \frac{\delta \rho_k h^3}{\eta_0 \kappa}. \quad (5)$$

Table 1
Symbols of the energy, momentum, and continuity Eqs. (1)–(3)

Symbol	Property	Definition	Value/unit
c_p	Heat capacity at constant pressure		$1250\,\mathrm{J\,kg^{-1}\,K^{-1}}$
Di	Dissipation number	$\frac{\alpha g h}{c_p}$	
e_{ij}	Strainrate tensor	$\partial_j u_i + \partial_i u_j$	$\mathrm{s^{-1}}$
g	Acceleration due to gravity		$3.71\,\mathrm{m\,s^{-2}}$
h	Length scale		1900×10^3 m
H	Radiogenic heat production		$\mathrm{W\,m^{-3}}$
p	Pressure		Pa
Δp	Dynamic pressure perturbation	$p - \rho_0 g z$	Pa
R	Internal heating number	$\frac{H_0 h^2}{\rho_0 c_p \kappa \Delta T}$	
Ra_H	Internal heating Rayleigh number	$\frac{\rho_0 g \alpha H h^5}{k \kappa \eta}$	
t	Time		s
T	Temperature		°C
T_0	Non-dimensional surface temperature		$\frac{273}{\Delta T}$
ΔT	Temperature scale		1600 °C
u	Velocity		$\mathrm{m\,s^{-1}}$
w	Vertical velocity		$\mathrm{m\,s^{-1}}$
z	Depth		m
α	Thermal expansion coefficient		$3 \times 10^{-5}\,\mathrm{K^{-1}}$
γ_k	Clapeyron slope	$\frac{\mathrm{d}P}{\mathrm{d}T}$	$\mathrm{Pa\,K^{-1}}$
Γ_k	Phase function	$\frac{1}{2}\left(1 + \sin\left(\pi \frac{z - z_0(T)}{\delta z}\right)\right)$	
$\delta\rho$	Phase density difference		$\mathrm{kg\,m^{-3}}$
η	Viscosity		Pa s
κ	Thermal diffusivity		$10^{-6}\,\mathrm{m^2\,s^{-1}}$
ρ_0	Reference density		$3416\,\mathrm{kg\,m^{-3}}$
τ_{ij}	Deviatoric stress tensor	ηe_{ij}	Pa
Φ	Viscous dissipation	ηe^2	$\mathrm{W\,m^{-3}}$

For the definitions of the other symbols, see Table 1. The convection is driven by internal heating, which decays with a halflife of 2 Gyr. Therefore, a suitable Rayleigh number to characterize the system is

$$Ra_H = \frac{\rho_0 g \alpha H h^5}{k \eta_0 \kappa}. \tag{6}$$

5.1. The dichotomy and lower mantle thickness

On Earth, the presence of a supercontinent may cause an accumulation of heat in the underlying mantle, thus influencing the dynamical and magmatic evolution of the planet (e.g., Yoshida et al., 1999). As the martian dichotomy shows a similarly striking difference in crustal thickness as Earth's distinction between continental and oceanic crust, and the thick southern hemisphere crust covers approximately half of the planet's surface, the dichotomy may be an important factor for the dynamics of the martian mantle. It is thought to have been formed very early in Mars' history (Frey et al., 2002; Solomon et al., 2005), so we assume it to be present at the start of our model calculations. It is included in a simple way in many of the models by prescribing a 100 km crust with an increased internal heating rate on the southern hemisphere. The bulk silicate Mars heating rate is assumed to be 4 times chondritic ($2 \times 10^{11}\,\mathrm{W\,kg^{-1}}$) at the start of the calculations, with a 20-fold concentration in the crust relative to the mantle. This results in all heat production being approximately equally partitioned between the two reservoirs, which is consistent with geochemical modeling suggesting that half of Mars' Nd budget resides in the crust (Norman, 1999).

As discussed above, the size of the martian core is still fairly ill constrained, but if present the lower mantle will not be thick. In our experiments, we apply a core size of 1497 km (corresponding to a 1900 km deep mantle), which, combined with the phase transition model described below, results in an initial lower mantle thickness of slightly less than 150 km.

5.2. Viscosity models and phase transitions

In two series of experiments, we first apply simple stratified models, and then add temperature and depth dependence of the viscosity. As the composition of the Earth's and the martian mantle are though to be rather similar (though the martian mantle is more iron-rich; Bertka and Fei, 1998), we assume its rheology to be similar as well. Glacial rebound studies (e.g., Lambeck et al., 1998) have suggested that the Earth's lower mantle is more than an order of magnitude stronger than the upper mantle. On the other hand, a recent theoretical model by Walzer et al. (2004) predicts a transition zone which is stronger than the upper mantle and the uppermost lower mantle. In case the lower mantle is hotter than the transition zone, a viscosity inversion may be expected. When assuming the lower mantle

Table 2
Parameter values used for the temperature and pressure dependent viscosity model, Eq. (7), based on Karato and Wu (1993)

Symbol	Property	Value
B	Prefactor	2.60×10^{10} Pa s
E	Activation energy	300 kJ mol^{-1}
V	Activation volume	6×10^{-6} m^3 mol^{-1}
R	Gas constant	8.341 J mol^{-1} K^{-1}

to be stronger than the upper mantle because of the different mineralogy, these effects may cancel out and the situation is approximated by an isoviscous model. When one assumes that the rheology of the transition zone and the lower mantle are similar, a temperature contrast results in a negative viscosity contrast, which is best represented by the strong transition zone model. We apply these results in our models in a simple manner by prescribing a viscosity prefactor with a value of 10 for either the transition zone or the lower mantle. As we assume these rheological transitions are associated with the phase transitions, described below, this prefactor is multiplied by the phase function Γ_k. This simple approximation reduces the required computation time relative to a fully temperature and pressure dependent rheology, allowing us to do a large number of numerical experiments and vary different parameters. To verify the results of the first series of experiments, we also consider the temperature and pressure dependence of the viscosity in some additional model runs, assuming diffusion creep to be dominant and ignoring dislocation creep. Following Karato and Wu (1993), we use the expression:

$$\eta = f(\Gamma_1, \Gamma_2) B \exp\left[\frac{E + pV}{RT}\right]. \quad (7)$$

Parameter values are listed in Table 2, assuming the values of Karato and Wu (1993) for a dry mantle.

In order to allow some kind of active surface tectonics to take place, we also run some experiments with temperature and pressure dependent viscosity in which the lithosphere of the northern hemisphere has a prescribed low viscosity, as an approximation of yielding behavior.

Additionally, in models where a thick southern hemisphere crust is included, the viscosity of this crust is prescribed ($10^3 \cdot \eta_0$) to prevent it from being swept away by the convecting mantle. The thickness of this crust corresponds quite well to the estimated thickness of the thermal lithosphere in early Mars (about 100 km; Hauck and Phillips, 2002) and therefore in the early Mars experiments, the crust and lithosphere are considered to be a single entity. The absence of a mechanical lithosphere on the northern hemisphere is an approximation to active surface tectonics.

Two solid state phase transitions are considered in our models. The first is the exothermic olivine–spinel transition, corresponding to the 400 km discontinuity in the Earth's mantle. We assume a commonly used value for the Clapeyron slope of $+3 \times 10^6$ Pa K^{-1} (Helffrich and Wood, 2001). The second transition taken into consideration is the γ-spinel-perovskite transition, representing the boundary between the upper and the lower mantle. The canonical value for the Clapeyron slope of this transition is about -3×10^6 Pa K^{-1} (e.g., Irifune et al, 1998; Hirose, 2002), but recent work by Katsura et al. (2003) suggests that the actual slope may be significantly less. Therefore, next to the classical value of -3×10^6 Pa K^{-1}, we also apply a value of -1×10^6 Pa K^{-1}.

The temperature of the martian mantle can be expected to vary by some hundreds of Kelvin during its evolution. For the Clapeyron slopes which are applied, this results in a upward (heating) or downward (cooling) movement of the perovskite phase transition on the order of 8–24 km per 100 K.

5.3. Discretization and boundary conditions

Equations (1)–(3) are solved on a 360° 2D cylindrical shell mesh of about 10^4 quadratic triangular elements (subdivided into linear elements for the energy equation). In the experiments, mesh refining is applied in the bottom ~300 km, resulting in a nodal point spacing of about 50 km in the upper mantle (35 km in additional resolution tests) and 25 km in the mesh refinement zone.

A second-order predictor–corrector scheme (Van den Berg et al., 1993) is used to integrate the energy equation in time. Particle tracers are used to prescribe the position of the southern hemisphere crust, and to monitor the advection of material from the deep mantle.

In order to purely study the effect of lower mantle flushing, an insulated lower boundary is prescribed to prevent the generation of plumes from a thermal boundary layer. The upper boundary has a fixed temperature of 0 °C. In the southern hemisphere crust models, no slip is prescribed for the southern hemisphere. The northern hemisphere boundary has either a free slip or a no slip condition, representing a plate tectonics like regime and a lower crust delamination regime, respectively, as alternatives for an active lid regime.

In the other models, free slip is prescribed on the entire top boundary.

6. Results

First we present a series of numerical experiments with a simple layered viscosity structure, which are used to determine the effects of viscosity stratification, mantle phase transitions, and the dichotomy on the passive formation of plume-like features (Section 6.1). The results of models with a temperature and pressure dependent rheology will be presented in Section 6.2.

6.1. Purely stratified viscosity models

The model experiments which were conducted with a purely layered viscosity model are listed in Tables 3 and 4. The resulting dynamics are summarized in these tables as well. The most important observation which can be distilled from Tables 3 and 4 is that an insulating raft on the southern hemisphere reduces the number of upwellings. The raft has a double function. Its increased internal heating rate and high viscosity cause

Table 3
Model experiments with distinguishing parameters and resulting upwelling characteristics

Model parameters						Results			
Run	Ra_H	s.h. raft	Mech. b.c.	γ_2 (MPa K^{-1})	Viscosity model	# upwel.	Initiation time (Myr)	Notes	Figure
0.1	1.1×10^8	–	fs	–	iso	6	100		Fig. 6a,b
0.3	1.1×10^8	√	fs	–	iso	2	<200[1]		Fig. 6c,d
1.1	1.1×10^8	–	fs	−1	iso	4–6	50–100	+	
1.2	1.1×10^8	–	fs	−1	LM	5	50–200		
1.3	1.1×10^8	–	fs	−1	TZ	4–6	50–100	+	
1.4	1.1×10^8	–	fs	−3	iso	4–6	50–100		Fig. 6e,f
1.5	1.1×10^8	–	fs	−3	LM	4–5	50–250		
1.6	1.1×10^8	–	fs	−3	TZ	4	50–100	+	
3.1	1.1×10^7	–	fs	−1	LM	3–5	500		
3.2	1.1×10^7	–	fs	−1	TZ	4–5	500	+	
3.3	1.1×10^7	–	fs	−3	LM	3–5	500		
3.4	1.1×10^7	–	fs	−3	TZ	4–6	500	+	

Notes. "s.h. raft" refers to the presence of a thick crust on the southern hemisphere. "Mech. b.c." refers to the type of mechanical boundary conditions (either free-slip or no-slip) on the outer boundary, or in the presence of a southern hemisphere raft, on the northern outer boundary only (the southern outer boundary always being no-slip in this case). In the viscosity model column, *iso*, *LM*, and *TZ* indicate experiments with a uniform viscosity, with a strong lower mantle, and with a strong transition zone, respectively. "# upwel." refers to the number of hot upwellings from the deep mantle produced *simultaneously* in the numerical experiment. The initiation time is defined here as the time required to develop full mantle scale upwellings from the lower mantle, as indicated by tracers in Figs. 6–8. The following symbols are used in the notes column of this and the next tables: + upwellings at right angles; NS northern hemisphere downwellings sweep hot material under southern hemisphere raft together to eventually form single upwelling.

[1] Total life span of focused upwelling activity.

Table 4
Model experiments with distinguishing parameters and resulting upwelling characteristics

Model parameters						Results			
Run	Ra_H	s.h. raft	Mech. b.c.	γ_2 (MPa K^{-1})	Viscosity model	# upwel.	Initiation time (Myr)	Notes	Figure
5.1	1.1×10^8	√	fs	−1	iso	1–2	100		
5.2	1.1×10^8	√	fs	−1	LM	1	100–200	NS	
5.3	1.1×10^8	√	fs	−1	TZ	1–2	100	NS	
5.4	1.1×10^8	√	fs	−3	iso	1–2	100		Fig. 6g,h
5.5	1.1×10^8	√	fs	−3	LM	1	100–200	NS	
5.6	1.1×10^8	√	fs	−3	TZ	2–3	100	NS	
7.1	1.1×10^7	√	fs	−1	LM	1	700–800	NS	
7.2	1.1×10^7	√	fs	−1	TZ	4 → 1	500	NS	
7.3	1.1×10^7	√	fs	−3	LM	1	700–800	NS	
7.4	1.1×10^7	√	fs	−3	TZ	4 → 1	500	NS	
9.1	1.1×10^7	√	ns	−1	iso	1–2	1300	NS	Fig. 7a,b
9.2	1.1×10^7	√	ns	−1	LM	1	1300	NS	Fig. 7e,f
9.3	1.1×10^7	√	ns	−1	TZ	4 → 2	1100	NS	Fig. 7c,d
9.4	1.1×10^7	√	ns	−3	iso	1	1300	NS	
9.5	1.1×10^7	√	ns	−3	LM	1	1300	NS	
9.6	1.1×10^7	√	ns	−3	TZ	4 → 2	1100	NS	
9.2b[1]	1.1×10^7	√	ns	−1	LM	1–2			
9.2.1	1.1×10^6	√	ns	−1	LM	1	≫1500		
9.2.2	1.1×10^8	√	ns	−1	LM	1	250	NS	
9.2.3	1.1×10^9	√	ns	−1	LM	1	<50	NS	

Note. See notes of Table 3 for further explanations.

[1] Continuation of experiment 9.2 at 500 Myr, with introduction of strong northern hemisphere crust.

a thermal blanketing effect which reduces the temperature contrast over the convecting mantle. And its mechanical coherency prevents cold downwellings from the surface to be formed. In most of the experiments with a southern hemisphere raft, we observe cold downwellings being formed in the northern hemisphere mantle. They tend to push hot deep mantle material towards the south, where they may form an upwelling. This mechanism is indicated in the last column of Table 4 (NS). Additional experiments have shown that when a strong lithosphere is also prescribed on the northern hemisphere, even when it is thinner than on the southern hemisphere, upwellings form under both hemispheres.

Please cite this article as: P. van Thienen et al., A top-down origin for martian mantle plumes, Icarus (2006), doi:10.1016/j.icarus.2006.06.008.

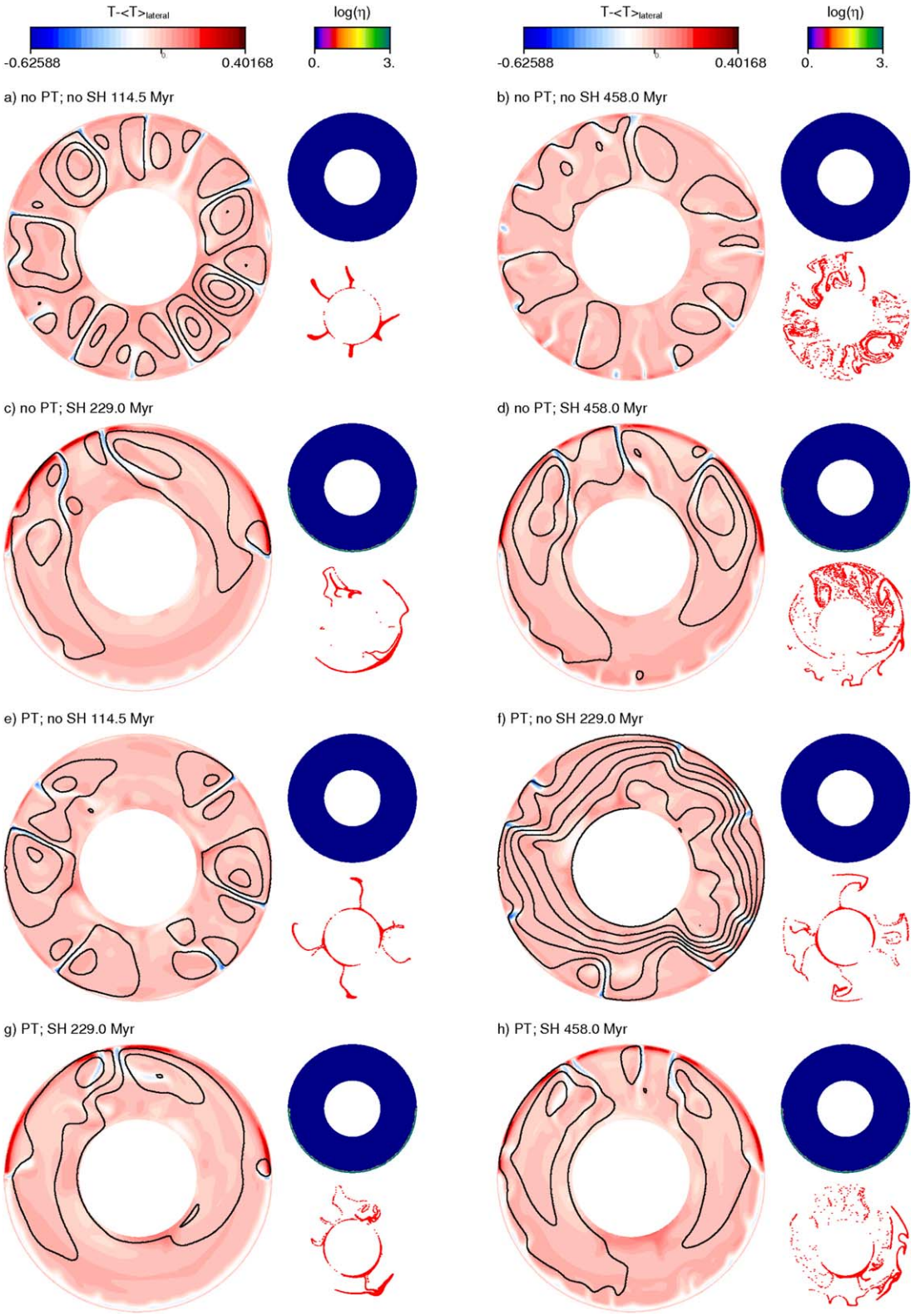

Fig. 6. Effects of phase transitions and a southern hemisphere raft on the convective pattern. Left frames show the deviation of the local temperature from the laterally averaged temperature. Upper right frames show the viscosity (in this figure only showing the raft if present), and the lower right frames show the location of tracers which were initially in the lower mantle. Two snapshots are shown for each of four different experiments, showing situations without phase transitions, excluding (a, b) and including a southern hemisphere raft (c, d), and with phase transitions excluding (e, f) and including a southern hemisphere raft (g, h). The results shown correspond to experiments from sets 0 (a, b, c, d), 1 (e, f), and 5 (g, h) in Table 3. The initial internal heating Rayleigh number is 1.1×10^8 in each case.

Please cite this article as: P. van Thienen et al., A top-down origin for martian mantle plumes, Icarus (2006), doi:10.1016/j.icarus.2006.06.008.

These results are illustrated in Fig. 6, which shows two snapshots for each of four numerical experiments with isoviscous mantles. The first case (Fig. 6a,b), with no phase transitions and no southern hemisphere raft, shows the formation of six more or less equally spaced upwellings of about equal strength, having cold downwellings in between. Adding a southern hemisphere raft (Fig. 6c,d) results in the generation of a single unfocused upwelling under the raft, balancing focused cold downwellings in the northern mantle. Fig. 6e,f (including phase transitions, no southern hemisphere raft) shows a focusing of upwellings from the deepest mantle. Their size is reduced relative to the numerical experiment without phase transitions (frames a, b), and so is the amount of material exchange between upper and lower mantle. Contrary to the case with a southern hemisphere raft and without phase transitions (frames c, d), the last case, which has both a raft and phase transitions shows continued focused upwelling in the southern mantle (frames g, h).

The time scales on which hot upwellings are formed strongly depend on the Rayleigh number. This is illustrated by models 9.2 and 9.2.1–9.2.3 (Table 4), which are identical apart from the Rayleigh number Ra_H. For $Ra_H = 1.1 \times 10^6$, no upwelling is formed on a relevant timescale. For increasing values, the time scale of upwelling formation rapidly decreases.

Another factor which appears to be important for the onset time of hot upwellings in our models is the mechanical boundary condition on the top boundary of the northern hemisphere. Comparison of equivalent models with free slip and no slip conditions (Table 4, models 7.1–7.4 versus models 9.1–9.2, 9.4–9.5) shows a difference of 500–800 Myr. The free slip and no slip models can be considered endmember cases of the active lid regime, the first approximating plate tectonics in a simple manner, and the latter being closer to crustal a delamination regime.

Fig. 7 shows the effects of viscosity stratification on the formation of a focused upwelling. Two snapshots of each of three models (isoviscous mantle: a, b; strong transition zone: c, d; strong lower mantle: e, f) demonstrate that viscosity stratification somewhat modulates the convective pattern, but is not a very important factor. Flushing of the lower mantle is more rapid in the first two cases (a, b, c, d) because of the lower viscosity in the lower mantle, but a truly focused upwelling takes some time to develop in each case. After about 1.5 billion years, one or two hot focused upwellings from the lower mantle are visible in each of the three cases (b, d, f) underneath the southern hemisphere raft.

6.2. Temperature and pressure dependent viscosity models

The relatively simple viscosity models applied in the previous section allow the running of a large number of numerical experiments to explore parameter space. To verify their applicability to Mars, we also did a number of experiments with more realistic rheology models (see Table 5). In the first of these, a temperature and pressure dependent rheology was applied, using expression (7). Two snapshots of the resulting temperature, flow field, viscosity and lower mantle tracers are shown in Fig. 8a,b. This rheology model results in a stagnant lid regime (Solomatov and Moresi, 1996). No strong cold downwellings are produced, and passive upwellings from the deep mantle are smaller, both in size and magnitude (by an order of magnitude), and numerous. The application of a weak northern hemisphere lithosphere (models 9.8–9.10), as an approximation to lithospheric yielding, however, does allow the formation of strong, cold downwellings from the surface in an active lid tectonic regime. Snapshots for model 9.8, exhibiting this specific regime, are shown in Fig. 8c,d. These frames show that the resulting dynamic regime is similar to that of numerical experiments with a simpler rheology model, as long as the southern hemisphere raft and phase transitions are included (see Table 4).

6.3. Long term stability of focused upwellings

We have performed additional experiments with a southern hemisphere raft, phase transitions, and a strong lower mantle, in which a strong northern hemisphere crust was added after an initial period of 500 Myr of active lid regime on the northern hemisphere, resulting in a reduction of the thermal amplitude of the cold downwellings generated here. Nevertheless, the initiation of downwellings in the northern hemisphere with a head start relative to the southern hemisphere results in a convection pattern which shows downwellings predominant in the northern mantle and a single focused upwelling underneath the southern hemisphere raft. This upwelling is stable for billions of years.

7. Discussion

We have presented an alternative mechanism for the generation and long term activity of large martian volcanic provinces

Table 5
Model experiments with temperature and pressure dependent rheology

Model parameters						Results			
Run	Ra_H	s.h. raft	Mech. b.c.	γ_2 (MPa K^{-1})	Viscosity model	# upwel.	Initiation time (Myr)	Notes	Figure
9.7	1.1×10^7	√	ns	−1	pT	4–5	1200		Fig. 8a,b
9.8	1.1×10^7	√	ns	−1	pTw	4 → 1	400	NS	Fig. 8c,d
9.9	1.1×10^7	√	ns	−1	pTw-LM	4 → 1	700	NS	
9.10	1.1×10^7	√	ns	−1	pTw-TZ	4 → 1	500	NS	

Notes. The rheology indications pT and pTw indicate a purely temperature and pressure dependent rheology without and with a weak northern hemisphere lithosphere, respectively. LM and TZ indicate an additional prefactor of 10 has been applied in the viscosity in the lower mantle and transition zone, respectively. For other explanations, see notes of Table 3.

Please cite this article as: P. van Thienen et al., A top-down origin for martian mantle plumes, Icarus (2006), doi:10.1016/j.icarus.2006.06.008.

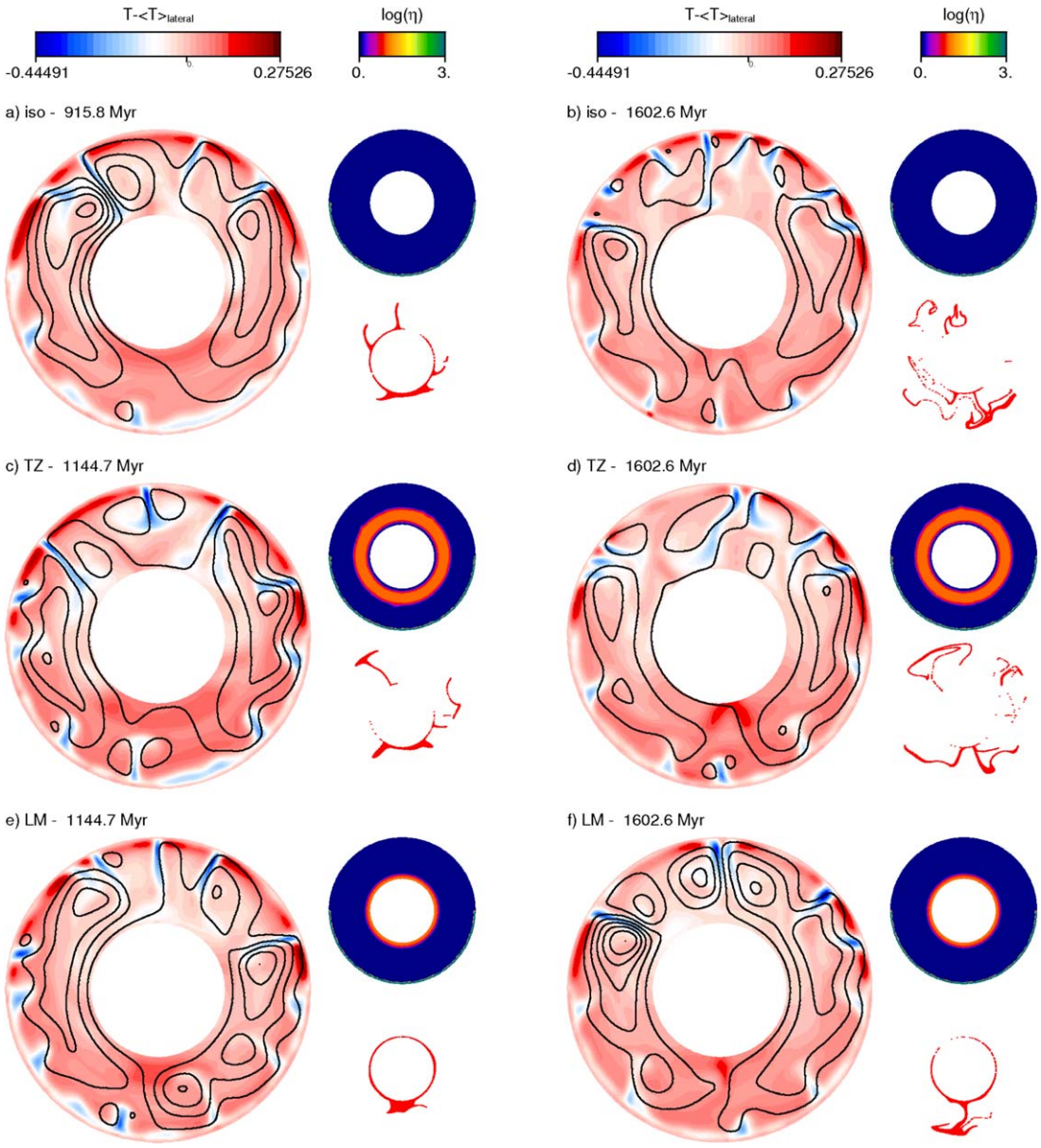

Fig. 7. Effects of viscosity stratification on the formation of a focused upwelling. Two snapshots of each of three models (isoviscous mantle: a, b; strong transition zone: c, d; strong lower mantle: e, f). For an explanation of figure setup and color scales, see the caption of Fig. 6. The results shown correspond to experiments from set 9 in Table 3. The initial internal heating Rayleigh number is 1.1×10^7 in each case.

and their stability, involving the flushing of the lower mantle. Three processes appear to be essential to the operation of this mechanism:

(1) The dichotomy, with a thick and stable crust and lithosphere on the southern hemisphere, and active lid tectonics on the northern hemisphere, divides the mantle into an active northern half and a more passive southern half.
(2) Cold downwellings generated in the northern hemisphere active lid regime penetrate into the lower mantle and displace hot material present there, which flows towards the southern hemisphere.
(3) The perovskite phase transition focuses the passively upwelling hot material into one or two upwellings.

These results are relatively insensitive to the Clapeyron slope of the perovskite phase transition. This mechanism provides a possible explanation for the early formation, stability, and long lived activity of the large volcanic provinces Tharsis and Elysium. It is also consistent with the presence of an active dynamo early in Mars' history (Nimmo and Stevenson, 2000). The timing of the formation of Tharsis is middle to late Noachian (Solomon et al., 2005). The experiments which best match this formation time are models 7.1–7.4 ($Ra_H = 1.1 \times 10^7$, free slip surface) and 9.8–9.10 ($Ra_H = 1.1 \times 10^7$, no slip surface), corresponding to a Rayleigh number of about $Ra_H = 10^7$.

It should be noted that our models more or less consistently show a possible discrepancy with Mars, which is the location of the upwellings relative to the positions of Tharsis and Ely-

Please cite this article as: P. van Thienen et al., A top-down origin for martian mantle plumes, Icarus (2006), doi:10.1016/j.icarus.2006.06.008.

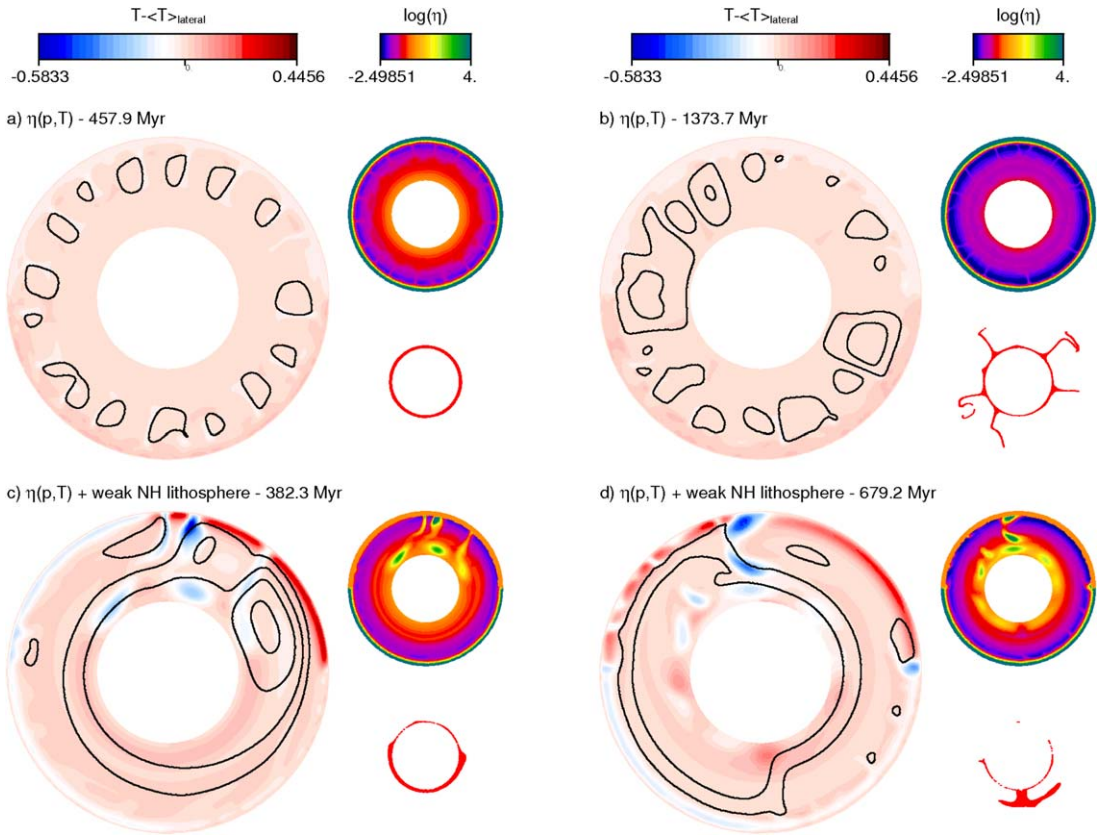

Fig. 8. Numerical experiments with temperature and pressure dependent rheologies excluding (a, b) and including (c, d) a weak northern hemisphere lithosphere.

sium. Whereas these volcanic provinces both have more or less equatorial positions, Tharsis appearing to be on the dichotomy boundary and Elysium in the northern hemisphere, the upwellings in our models favor formation well underneath the southern hemisphere.

The two main uncertainties regarding our model are the size of the martian core, i.e., the question whether Mars actually has a lower mantle, and the question to what extent an active lid regime was active on the martian northern hemisphere during the planet's early history, and if so, why it shut down. Concerning the first question, this will not really be answered until we put seismometers on Mars, but we have demonstrated that Mars interior models with a thin lower mantle may be constructed that are consistent with presently available data.

The question of an active lid regime on the northern hemisphere has been addressed by other authors. Sleep (1994) interpreted the geology of the northern hemisphere in terms of a plate tectonic origin. Similarly, Connerney et al. (1999) interpreted magnetic striping found in the southern highlands as possibly having a plate tectonic origin. Lenardic et al. (2004) considered the convective stresses in the martian mantle during the planet's evolution. They found that a mobile lid regime such as plate tectonics may have coexisted with a laterally growing thick southern hemisphere crust (assumed to be stable due to its intrinsic chemical buoyancy) for some time. Their model shows that the mantle heats up as the extent of the insulating southern hemisphere crust grows, reducing the mantle viscosity and stresses associated to convection. At some point, stresses drop below the lithosphere yield stress, and the mobile lid regime is terminated. However, calculations of thermochemical buoyancy by Van Thienen et al. (2004b) showed that it is very difficult to produce a lithosphere on Mars at a mid-ocean ridge which will develop a negative buoyancy, because of the thick crust and depleted root which are produced in the reduced martian gravity field. In other words, martian oceanic lithosphere would be very difficult to subduct. Breuer and Spohn (2003) conclude on the basis of parametric mantle convection models that an early phase of plate tectonics on Mars is unlikely, because the associated crustal growth curve does not sufficiently match the monotonically declining planetary crustal growth rate which is observed.

Therefore, the required active lid regime on the martian northern hemisphere was probably not plate tectonics as it is taking place on the present-day Earth. Alternatives may include large-scale delamination of the lower crust, or episodic subduction (Stein et al., 2004; Van Thienen et al., 2004a) rather than the continuous plate tectonics process. Also, as pointed out by Lenardic et al. (2004), an active lid regime with more diffuse zones of deformation can be imagined.

Our results are reasonably similar to those of Harder (1998), but the structures develop on a much smaller timescale in our models. The most important difference between the model setups (apart from the 2/3D question) are the presence of a dichotomy in our models, and the higher Rayleigh numbers used here. Whereas Harder's two plume regime requires several billion years to be formed (ascribed to the absence of decay of

Please cite this article as: P. van Thienen et al., A top-down origin for martian mantle plumes, Icarus (2006), doi:10.1016/j.icarus.2006.06.008.

heat sources in the model), in some of our models this may take place in several hundred million years, which appears more realistic considering the age of the volcanic provinces. The higher Rayleigh numbers of our models relative to those of Harder partly explain the shorter time scales we find. The 'imposition' of the convective pattern (downwellings in the northern mantles and upwellings in the southern mantle) by the dichotomy may also reduce the time required to evolve from the initial state to the single our double upwelling mode. Harder (1998) reported that a predominantly internally heated mantle (only 10% basal heating) also produced this type of dynamics. Our results go one step further in indicating that basal heating is not required at all.

8. Concluding remarks

The results presented in this paper demonstrate that flushing of the lower mantle is a viable mechanism for the generation of the large volcanic provinces Tharsis and Elysium on Mars. Essential ingredients are the dichotomy, the early operation of an active lid regime on the northern hemisphere, and the perovskite phase transition in the deep mantle.

Acknowledgments

We thank Walter J. Kiefer and Chris Reese for constructive reviews which helped to improve and clarify the paper, and Ruth Ziethe for a discussion concerning core formation. Peter van Thienen acknowledges the financial support provided through the European Community's Human Potential Programme under contract RTN2-2001-00414, MAGE. Calculations were done at the Département de Modélisation Numérique et Physique at IPGP. This is IPGP contribution No. 2142.

References

Abe, Y., 1997. Thermal and chemical evolution of the terrestrial magma ocean. Phys. Earth Planet. Inter. 100, 27–39.

Acuña, M.H., Connerney, J.E.P., Ness, N.F., Lin, R.P., Mitchell, D., Carlson, C.W., McFadden, J., Anderson, K.A., Rème, H., Mazelle, C., Vignes, D., Wazilewsky, P., Cloutier, P., 1999. Global distribution of crustal magnetization discovered by the Mars Global Surveyor MAG/ER experiment. Science 284 (5415), 790–793.

Anderson, D.L., 2002. The case for irreversible chemical stratification of the mantle. Int. Geol. Rev. 44, 97–116.

Anderson, D.L., Tanimoto, T., Zhang, Y.-S., 1992. Plate tectonics and hotspots: The third dimension. Science 256, 1645–1651.

Balmino, G., Duron, J., Marty, J.C., Karatekin, Ö., 2005. Mars long wavelength gravity field time variations: A new solution from MGS tracking data. In: Dynamic Planet 2005. IAG-IAPSO-IABO Joint Scientific Assembly, Cairns, Australia, August 22–26, 2005.

Bertka, C.M., Fei, Y., 1997. Mineralogy of the martian interior up to core-mantle boundary pressures. J. Geophys. Res. 102, 5251–5264.

Bertka, C.M., Fei, Y., 1998. Density profile of an SNC model martian interior and the moment-of-inertia factor of Mars. Earth Planet. Sci. Lett. 157, 79–88.

Breuer, D., Spohn, T., 2003. Early plate tectonics versus single-plate tectonics on Mars: Evidence from magnetic field history and crust evolution. Geophys. Res. 108 (E7), doi:10.1029/2002JE001999.

Breuer, D., Yuen, A.D., Spohn, T., 1997. Phase transitions in the martian mantle: Implications for partially layered convection. Earth Planet. Sci. Lett. 148, 457–469.

Christensen, U.R., Yuen, D.A., 1985. Layered convection induced by phase transitions. J. Geophys. Res. 99, 10291–10300.

Connerney, J.E.P., Acuña, M.H., Wasilewski, P.J., Ness, N.F., Rème, H., Mazelle, C., Vignes, D., Lin, R.P., Mitchell, D.L., Cloutier, P.A., 1999. Magnetic lineation in the ancient crust of Mars. Science 284, 794–798.

Cserepes, L., Yuen, D.A., 2000. On the possibility of a second kind of mantle plume. Earth Planet. Sci. Lett. 183, 61–71.

Dohm, J.D., Tanaka, K.L., 1999. Geology of the Thaumasia region, Mars: Plateau development, valley origins, and magmatic evolution. Planet. Space Sci. 47, 411–431.

Dreibus, G., Wänke, H., 1985. Mars, a volatile-rich planet. Meteoritics 20, 367–381.

Elkins-Tanton, L.T., Parmentier, E.M., Hess, P.C., 2003. Magma ocean fractional crystallization and cumulate overturn in terrestrial planets: Implications for Mars. Meteorit. Planet. Sci. 38 (12), 1753–1771.

Folkner, W.M., Yoder, C.F., Yuan, D.N., Standish, E.M., Preston, R.A., 1997. Interior structure and seasonal mass redistribution of Mars from radio tracking of Mars Pathfinder. Science 278, 1749–1751.

Frey, H.V., Roark, J.H., Shockey, K.M., Frey, E.L., Sakimoto, S.E.H., 2002. Ancient lowlands on mars. Geophys. Res. Lett. 29 (10), doi:10.1029/2001GL013832.

Halliday, A.N., Wänke, H., Birck, J., Clayton, R.N., 2001. The accretion, composition and early differentiation of Mars. Space Sci. Rev. 96, 197–230.

Harder, H., 1998. Phase transitions and three-dimensional planform of thermal convection in the martian mantle. J. Geophys. Res. 103 (E7), 16775–16797.

Harder, H., Christensen, U., 1995. A one-plume model of martian mantle convection. Nature 380, 507–509.

Hartmann, W.K., Malin, M., McEwen, A., Carr, M., Soderblom, L., Thomas, P., Danielson, E., James, P., Veverka, J., 1999. Evidence for recent volcanism on Mars from crater counts. Nature 397, 586–589.

Hauck, S.A.I., Phillips, R.J., 2002. Thermal and crustal evolution of Mars. J. Geophys. Res. 107 (E7), doi:10.1029/2001JE001801.

Helffrich, G.R., Wood, B.J., 2001. The Earth's mantle. Nature 412, 501–507.

Hirose, K., 2002. Phase transitions in pyrolitic mantle around 670-km depth: Implications for upwelling of plumes from the lower mantle. J. Geophys. Res. 107 (B4), doi:10.1029/2001JB000597.

Irifune, T., Nishiyama, N., Koruda, K., Inoue, T., Isshiki, M., Utsumi, W., Funakoshi, K., Urakawa, S., Uchida, T., Katsura, T., Ohtaka, O., 1998. The postspinel phase boundary in Mg_2SiO_4 determined by in situ X-ray diffraction. Science 279, 1698–1700.

Karato, S.-i, Wu, P., 1993. Rheology of the upper mantle: A synthesis. Science 260, 771–778.

Katsura, T., Yamada, H., Shinmei, T., Kubo, A., Ono, S., Kanzaki, M., Yoneda, A., Walter, M.J., Ito, E., Urakawa, S., Funakoshi, K., Utsumi, W., 2003. Post-spinel transition in Mg_2SiO_4 determined by high P–T in situ X-ray diffractometry. Phys. Earth Planet. Inter. 136, 11–24.

Kiefer, W.S., 2003. Melting in the martian mantle: Shergottite formation and implications for present-day mantle convection on Mars. Meteorit. Planet. Sci. 39 (12), 1815–1832.

Konopliv, A.S., Yoder, C.F., Standish, E.M., Yuan, D., Sjogren, W.L., 2006. A global solution for the Mars static and seasonal gravity, Mars orientation, Phobos and Deimos masses, and Mars ephemeris. Icarus 182, 23–50.

Lambeck, K., Smither, C., Johnston, P., 1998. Sea-level change, glacial rebound and mantle viscosity for northern Europe. Geophys. J. Int. 134, 102–144.

Lenardic, A., Nimmo, F., Moresi, L., 2004. Growth of the hemispheric dichotomy and the cessation of plate tectonics on Mars. J. Geophys. Res. 109 (E02003), doi:10.1029/2003JE002172.

Longhi, J., Knittle, E., Holloway, J.R., Wänke, H., 1992. The bulk composition, mineralogy and internal structure of Mars. In: Kieffer, H.H., Jakowsky, B.M., Snyder, C.W., Mathews, M.S. (Eds.), Mars. Univ. of Arizona Press, Tucson, pp. 184–208.

Machetel, P., Weber, P., 1991. Intermittent layered convection in a model mantle with an endothermic phase change at 670 km. Nature 350, 55–57.

Neukum, G., Jaumann, R., Hoffmann, H., Hauber, E., Head, J.W., Basilevsky, A.T., Ivanov, B.A., Werner, S.C., van Gasselt, S., Murray, J.B., McCord, T.,

The HRCS Co-Investigator Team, 2004. Recent and episodic volcanic and glacial activity on Mars revealed by the High Resolution Stereo Camera. Nature 432, 971–979.

Nimmo, F., Stevenson, D.J., 2000. Influence of early plate tectonics on the thermal evolution and magnetic field of Mars. J. Geophys. Res. 105 (E5), 11969–11979.

Norman, M.D., 1999. The composition and thickness of the crust of Mars estimated from rare Earth elements and neodymium-isotopic compositions of martian meteorites. Meteorit. Planet. Sci. 34, 439–449.

Reese, C.C., Solomatov, V.S., Baumgardner, J.R., Stegman, D.R., Vezolainen, A.V., 2004. Magmatic evolution of impact-induced martian mantle plumes and the origin of Tharsis. J. Geophys. Res. 109 (E08009), doi:10.1029/2003JE002222.

Righter, K., Hervig, R.L., Kring, D.A., 1998. Accretion and core formation on Mars: Molybdenum contents of melt inclusion glasses in three SNC meteorites. Geochim. Cosmochim. Acta 62 (12), 2167–2177.

Sanloup, C., Jambon, A., Gillet, P., 1999. A simple chondritic model of Mars. Phys. Earth Planet. Inter. 112, 43–54.

Schubert, G., Bercovici, D., Glatzmaier, G.A., 1990. Mantle dynamics in Mars and Venus: Influence of an immobile lithosphere on three-dimensional mantle convection. J. Geophys. Res. 95 (B9), 14105–14129.

Schumacher, S., Breuer, D., 2006. Influence of a variable thermal conductivity on the thermo-chemical evolution of Mars. J. Geophys. Res. 111 (E02006), doi:10.1029/2005JE002429.

Segal, A., Praagman, N.P., 2002. The Sepran Package. Technical report. http://ta.twi.tudelft.nl/sepran/sepran.html.

Senchu, H., Kuramoto, K., Matsui, T., 2002. Thermal evolution of a growing Mars. J. Geophys. Res. 107 (E12), doi:10.1029/2001JE001819.

Sleep, N.H., 1994. Martian plate tectonics. J. Geophys. Res. 99 (E3), 5639–5655.

Smith, D.E., Zuber, M.T., Neumann, G.A., 2001. Seasonal variations of snow depth on Mars. Science 294 (5549), 2241–2246.

Sohl, F., Schubert, G., Spohn, T., 2005. Geophysical constraints on the composition and structure of the martian interior. J. Geophys. Res. 110 (E12008), doi:10.1029/2005JE002520.

Sohl, F., Spohn, T., 1997. The interior structure of Mars: Implications from SNC meteorites. J. Geophys. Res. 102, 1613–1636.

Solomatov, V.S., 2000. Fluid dynamics of a terrestrial magma ocean. In: Canup, R., Righter, K. (Eds.), Origin of the Earth and Moon. Univ. Arizona Press, Tuscon, pp. 323–338.

Solomatov, V.S., Moresi, L.-N., 1996. Stagnant lid convection on Venus. J. Geophys. Res. 101 (E2), 4737–4753.

Solomon, S.C., Aharonson, O., Aurnou, J.M., Banerdt, W.B., Carr, M.H., Dombard, A.J., Frey, H.V., Golombek, M.P., Hauck, S.A.I., Head, J.W.I., Jakosky, B.M., Johnson, C.L., McGovern, P.J., Neumann, G.A., Phillips, R.J., Smith, D.E., Zuber, M.T., 2005. New perspectives on ancient Mars. Science 307, 1214–1220.

Stein, C., Schmalzl, J., Hansen, U., 2004. The effect of rheological parameters on plate behavior in a self-consistent model of mantle convection. Phys. Earth Planet. Inter. 142, 225–255.

Tackley, P.J., Stevenson, D.J., Glatzmaier, G.A., Schubert, G., 1993. Effects of an endothermic phase transition at 670 km depth in spherical model of convection in Earth's mantle. Nature 361, 699–703.

Van den Berg, A.P., Van Keken, P.E., Yuen, D.A., 1993. The effects of a composite non-Newtonian and Newtonian rheology on mantle convection. Geophys. J. Int. 115, 62–78.

Van Thienen, P., Van den Berg, A.P., Vlaar, N.J., 2004a. Production and recycling of oceanic crust in the early Earth. Tectonophysics 386 (1–2), 41–65.

Van Thienen, P., Vlaar, N.J., Van den Berg, A.P., 2004b. Plate tectonics on the terrestrial planets. Phys. Earth Planet. Inter. 142 (1–2), 61–74.

Verhoeven, O., Rivoldini, A., Vacher, P., Mocquet, A., Choblet, G., Menvielle, M., Dehant, V., Van Hoolst, T., Sleewaegen, J., Barriot, J.-P., Lognonné, P., 2005. Interior structure of terrestrial planets: Modeling Mars' mantle and its electromagnetic, geodetic, and seismic properties. J. Geophys. Res. Planets 110 (E9). 4009.

Walzer, U., Hendel, R., Baumgardner, J., 2004. The effects of a variation of the radial viscosity profile on mantle evolution. Tectonophysics 384 (1–4), 55–90.

Weinstein, S.A., 1995. The effects of a deep mantle endothermic phase change on the structure of thermal convection in silicate planets. J. Geophys. Res. 100 (E6), 11719–11728.

Wenzel, M.J., Manga, M., Jellinek, A.M., 2004. Tharsis as a consequence of Mars' dichotomy and layered mantle. Geophys. Res. Lett. 31 (L04702), doi:10.1029/2003GL019306.

Williams, J.-P., Nimmo, F., 2004. Thermal evolution of the martian core: Implications for an early dynamo. Geology 32 (2), doi:10.1130/G19975.1, 97–100.

Yoder, C.F., Konopliv, A.S., Yuan, D.N., Standish, E.M., Folkner, W.M., 2003. Fluid core size of Mars from detection of the solar tide. Science 300, 299–303.

Yoder, C.F., Konopliv, A.S., Yuan, D.N., Standish, E.M., Folkner, W.M., 2003. Fluid core size of Mars from detection of the solar tide. Science 300, 299–303.

Yoshida, M., Iwase, Y., Honda, S., 1999. Generation of plumes under a localized high viscosity lid in 3-D spherical shell convection. Geophys. Res. Lett. 26 (7), 947–950.

Zuber, M.T., 2001. The crust and mantle of Mars. Nature 412, 220–227.

Please cite this article as: P. van Thienen et al., A top-down origin for martian mantle plumes, Icarus (2006), doi:10.1016/j.icarus.2006.06.008.